Polymer 50 (2009) 5076–5083

Contents lists available at ScienceDirect

Polymer

journal homepage: www.elsevier.com/locate/polymer

A ToF-SSIMS study of plasma polymer-based patterned metal affinity surfaces

Gregory J.S. Fowler [a,1], Gautam Mishra [a,1,2], Christopher D. Easton [b], Sally L. McArthur [b,*]

[a] Department of Engineering Materials, The Kroto Research Institute, University of Sheffield, Broad Lane, Sheffield S3 7HQ, UK
[b] Biointerface Engineering Group, IRIS, Faculty of Engineering and Industrial Sciences, Swinburne University of Technology, Hawthorn, Victoria, Australia

ARTICLE INFO

Article history:
Received 10 July 2009
Received in revised form
31 August 2009
Accepted 2 September 2009
Available online 6 September 2009

Keywords:
Plasma polymer
ToF-SSIMS
Metal affinity

ABSTRACT

Polymers that exhibit an affinity to metal ions are important for separation science and sensor applications. In this paper, we describe the creation of surface micropatterns with three plasma polymers, acrylic acid (ppAAc), allylamine (ppAAm) and tetraglyme (ppTG). Time-of-Flight Static Secondary Ion Mass Spectrometry (ToF-SSIMS) imaging has been used to visualise the chemical specificity and selectivity of the plasma polymers as substrates for immoblised metal affinity protein separation. This technique provides the necessary spatial resolution to chemically resolve the multiple components present on these surfaces. Enzyme-linked immunosorbent assay (ELISA) was also employed to confirm the biological specificity of these surfaces. The results clearly demonstrate that under the correct solvent conditions, ppAAc-modified surfaces coordinate gallium and are able to selectively attract phosphoproteins. Critically, it is possible to then remove the protein from the surface and regenerate the chemistry using a simple elevated pH washing step. These results indicate the potential of these surfaces for implementation in microfluidic devices for the rapid isolation or pre-concentration of phosphopeptides/proteins.

1. Introduction

Plasma polymers have become increasingly popular for the creation of surfaces for use in biological environments involving living cells and proteins [1–3]. Plasma polymerisation is capable of producing a range of surface chemical functionalities independent of the substrate chemistry, with film thicknesses that can be controlled on the nanometre scale. Since plasma polymers can coat a variety of surface geometries exposed to the plasma phase, they are naturally useful in the construction of microfluidic devices for biomedical applications. In previous studies we have shown that plasma polymers can be used to create protein resistant coatings in composite microfluidic devices constructed from glass and teflon [4] and improve cell attachment to electrospun scaffolds for tissue engineering nerve guides [5].

The ability to fabricate surface chemistries that demonstrate an affinity to metal ions provides a number of exciting research opportunities. Immobilised metal affinity chromatography (IMAC) [6] is a common technique employed in protein separation that exploits the affinity of proteins to certain metal ions. It is a commonly used method for the selective enrichment of phosphoproteins. Post-translational protein phosphorylation is critical in the initiation and control of signal transduction pathways that regulate the proliferation, migration and differentiation of cells, and is therefore of particular interest in proteomics [7]. Phosphoproteins are immobilised onto a stationary phase via electrostatic interactions of the phosphate groups with positively charged metal ions (Fe^{3+}, Ga^{3+}) [8,9], coupled to the stationary material via nitrilotriacetic acid (NTA), iminodiacetic acid (IDA) or tris-(carboxymethyl)-ethylenediamine (TED) chelators [6] or alternately via the metal oxides of titanium or zirconium [10,11]. Co-retention of peptides/proteins containing phosphorylated and acidic residues, together with a limited retention of specific phosphopeptides, can restrict the general utility of phospho-IMAC. Care needs to be taken to choose suitable solvent systems that favour the immobilisation of phosphoserine and phosphotyrosine whilst suppressing the immobilisation of amino acids such as glutamic acid or aspartic acid that have acidic ionizable side-chains [8,9]. This can be achieved by a combination of low pH, which leaves phosphate as the main negatively charged species in the peptide/protein, and the use of semi-organic solvents which suppress the remaining negative charges due to acidic protein residues [9,12,13]. Integration of IMAC techniques into microfluidic devices using metal affinity surfaces would provide improvements over existing techniques. Microfluidic analytical techniques use reagent volumes

* Corresponding author. Tel.: +61 03 9214 8452; fax: +61 03 9214 5050.
E-mail address: smcarthur@groupwise.swin.edu.au (S.L. McArthur).
[1] Joint first authors.
[2] Present Address: Kratos Analytical, Wharfside, Trafford Wharf Road, Manchester M17 1GP, UK.

0032-3861/$ – see front matter © 2009 Elsevier Ltd. All rights reserved.
doi:10.1016/j.polymer.2009.09.005

many times smaller than conventional experiments, reducing sample requirements and analysis times, and proving much more efficient than, for example, gel-based methodologies [14,15]. An adaptation of IMAC suitable for incorporation into a microfluidic device can fulfil many of these criteria, but a key challenge lies in developing surface modification strategies for microfluidic devices that are robust and flexible, without the complexity of packing the channels with the more traditional bead supports [16,17]. Another potential direction for metal affinity surfaces is the sensor industry. An example has been demonstrated by Cooper et al. [18], where a chelating polymer coating with an affinity for 2+ metal-ion was integrated into an optical fibre in order to perform corrosion sensing in aircraft.

Plasma polymerisation of acrylic acid (ppAAc) produces coatings with carboxylic acid functionality [19], which are the chelating groups found in NTA and IDA [6,20]. In this paper, we describe the creation of surface micropatterns with three plasma polymers, ppAAc, allylamine (ppAAm) and tetraglyme (ppTG) in order to study the specificity and selectivity of plasma polymers as immobilised metal affinity supports. ppAAc gives an acid rich surface, ppAAm produces an amine rich surface, while ppTG produces a PEO-like surface that resists protein adsorption [4,21]. We have then studied their behaviour when exposed to gallium salts and whole proteins under controlled solvent conditions. The use of micropatterns allows visualisation and direct comparison of the interactions with different surface chemistries on the micron-scale. Time-of-Flight Static Secondary Ion Mass Spectrometry (ToF-SSIMS) is a powerful surface science technique that provides the necessary spatial resolution to chemically resolve these micropatterns and is able to distinguish between the polymer, bound metal ions and proteins. ToF-SSIMS spectroscopy and imaging were used to examine co-localisation properties of gallium and phopsphorylated proteins on the plasma polymer micropatterns. Enzyme-linked immunosorbent assay (ELISA) measurements were then used to biochemically establish the level of the surface immobilised phosphoprotein.

The results of these studies clearly demonstrate that different microarrays of plasma polymers can be produced and used to create immobilised metal affinity regions capable of selecting proteins from solution via phospho-Ga interactions. The ability to subsequently release the captured protein from the surface and regenerate the surface means that this approach has potential as a coating for microfluidic devices and a wide range of other materials where metal affinity is required.

2. Experimental

2.1. Materials

Gallium (III) nitrate xH_2O (Sigma), Acrylic acid ($CH_2=CHCOOH$, Aldrich), Allylamine ($CH_2=CHCH_2NH_2$, Aldrich), Tetraglyme (Tetraethylene glycol dimethyl ether, $CH_3O(CH_2CH_2O)_4CH_3$, Aldrich), silicon wafers (Orientation: <100>, Thickness; 525 microns, Dopants: P.Boron, Resistivity: 1–10 Ohm cm, Polish: one side, Compart Technology Ltd.), Glass coverslips (round 13 mm, thickness 1.5 mm, VWR International Ltd.), O-phosphoserine-L-BSA (PLS-BSA) phosphoprotein (Sigma), Rabbit anti-phosphoserine-BSA-HRP (polyclonal, Abcam), AZ 1512 Photoresist (MicroChemicals GmbH), AZ 351B Developer (MicroChemicals, GmbH).

2.2. Plasma polymerisation

Prior to plasma polymerisation, each of the monomers was degassed several times using freeze thaw cycles. All substrates used in the experiments were sonicated in isopropanol prior to use.

2.2.1. Acrylic acid

The conditions under which acid functional plasma polymer coatings were deposited using an acrylic acid precursor has been explained in detail elsewhere [19]. Briefly, the plasma polymerisation took place in a cylindrical glass reactor (10 cm diameter and 50 cm long). The reactor was connected to a vacuum pump and an in-line liquid nitrogen cold-trap. A radio frequency power source (13.56 MHz, Coaxial Power Systems Ltd., UK) was coupled to the reactor via an impedance matching unit, delivered through a copper coil wound externally around the glass reactor. The substrates were placed in the "in-coil" region of the reactor and the vessel was pumped down to a base pressure of 1×10^{-3} mbar. Deposition power, time and monomer flow rate were fixed at 10 W, 15 min and 2.0 sccm respectively.

2.2.2. Allylamine

An amine functionalised surface was generated using an allylamine monomer precursor. The experimental setup has been explained in detail elsewhere [22]. Briefly a T-piece cylindrical glass reactor of 10 cm internal diameter and 40 cm length was used. Radio frequency power was coupled to the plasma reactor via an impedance matching unit and externally wound turns of insulated copper wire. Substrates were placed in the centre of the reactor, and the vessel was pumped down to a pressure of less than 1×10^{-3} mbar. Deposition power, time and monomer flow rate were fixed at 10 W, 15 min and 2.0 sccm respectively.

2.2.3. Tetraglyme

The PEO-like ether-carbon rich non-fouling plasma polymer films were created using tetraglyme as the monomer. The experimental setup has been explained in detail elsewhere [4]. Briefly, a stainless steel T-piece reactor was used whilst the power from an RF generator was fed to the internal aluminium disc electrode via an electrical feed-through, while the rest of the stainless steel chamber was grounded. The radio frequency power source (13.56 MHz, Coaxial Power Systems Ltd., UK) was coupled to the reactor via an impedance matching unit. The substrates were placed in the reactor and the vessel was pumped down to a base pressure of 1×10^{-3} mbar. Due to the low volatility of tetraglyme monomer, both the reactor chamber and the monomer were heated to 55 and 95 °C respectively. Deposition power, time and monomer flow rate were fixed at 10 W, 25 min and 2.5 sccm respectively.

2.3. Photolithographic surface patterning

The process of patterning plasma polymers using photolithography was adapted from the methods of Goessl et al. [23]. The positive photoresist (AZ 1512, MicroChemicals GmbH) was spin coated at 4000 rpm onto the base plasma polymer and a uniform 1–1.5 μm thickness coating obtained. The wafers were then heated to 90 °C for 120 s to remove the remaining solvent and harden the resist. The photolithographic pattern was formed by bringing the resist-coated silicon wafer into intimate contact with an optical photomask and exposing it to ultraviolet radiation (Electronic Vision A16-2 mask aligner) for 5 s. The light-exposed photoresist was removed by immersion of the sample in an alkaline developer (AZ 351B, MicroChemicals, GmbH) at a dilution ratio of 1:4 (developer: water) for 30 s. The samples were then rinsed several times with ultra pure water and dried in a stream of nitrogen, ready for the deposition of the second plasma polymer layer. The second polymer layer was then deposited on top of the base layer polymer and photoresist pattern. Once both plasma polymers were in place, the remaining photoresist was dissolved by immersing the samples in a solution of acetone and sonicating them for 3×20 s. During the removal process, the polymer deposited on top of the patterned

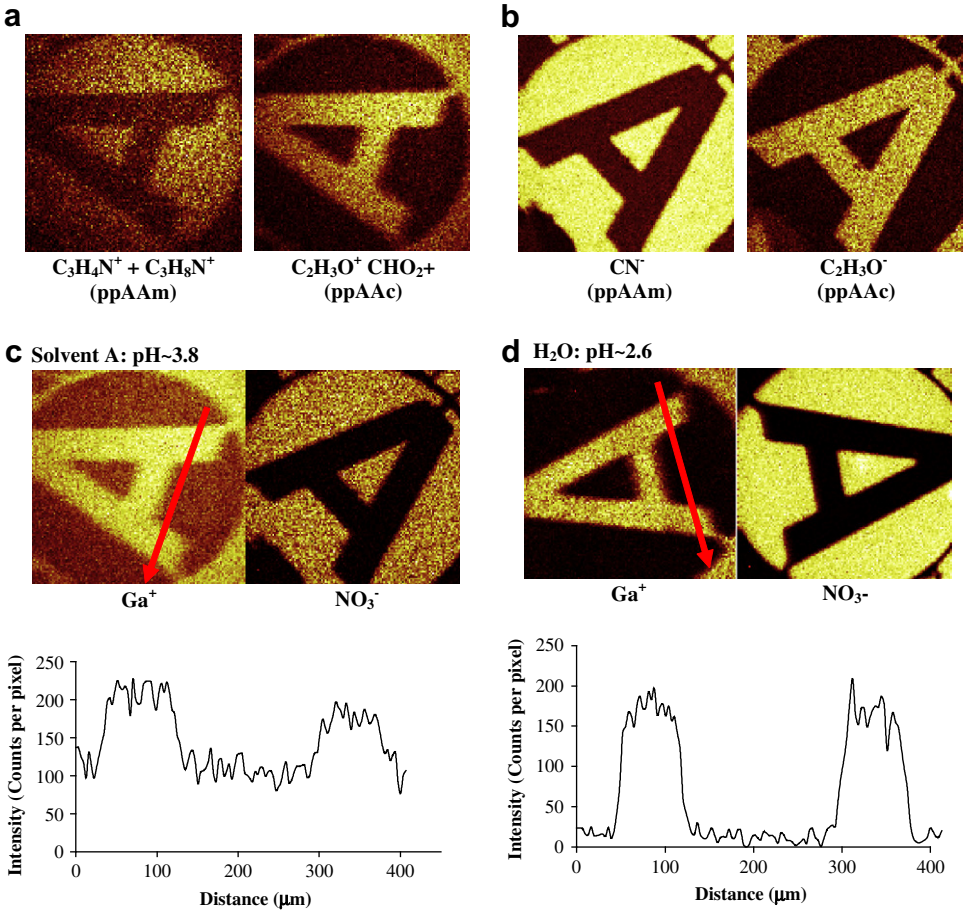

Fig. 1. (a) Positive and (b) negative ToF-SSIMS images of ppAAc/ppAAm micropatterns on a silicon wafer, showing the resolution of various chemical species associated with the two plasma polymers. (Field of view of each square panel = 500 × 500 microns.) **(c)** and **(d)** The effect of the solvent on the localisation of gallium and nitrate ions associated with the surface. Metal salt solutions were either buffered 20 mM gallium nitrate (Solvent A, 0.1 M sodium acetate/1 M NaCl, pH 4.0 – see text) or non-buffered 20 mM gallium nitrate (ddH_2O, pH ~2.8). The line scans shown below represent the intensity variation along the red arrows superimposed on the TOF-SSIMS images, both with respect to the length and the direction.

resist (thus the polymer adhered to the resist) was also removed, creating the dual plasma polymer pattern. The samples were then extensively washed with MiliQ grade water and dried under a stream of nitrogen. Micropatterns of ppTG/ppAAc, ppAAc/ppAAm and ppTG/ppAAm were produced for this study. In this nomenclature for the samples, the first named plasma polymer forms the base layer or background of the coating.

2.4. Surface characterisation using ToF-SSIMS

ToF-SSIMS spectra and images were obtained using a ToF SIMS V instrument (ION TOF Inc. Munster, Germany). The analysis chamber was held at -1×10^{-8} mbar during experiments. The primary ion beam was generated using a liquid metal ion gun fitted with a pure bismuth ion source capable of producing Bi_n^{p+} ($n = 1$–6, $p = 1$–2) ions. The kinetic energy of these ions was 25 keV for singly charged ions and 50 keV for doubly charged ions. The angle of incidence of the primary ion beam relative to the sample surface was 45°. Bi_3^{2+} primary ion source was used for all image and spectral data acquisition. The primary ion currents, measured using a Faraday cup located on the grounded sample holder, were typically around −0.1 pA (Bi_3^{2+}) at 10 kHz.

Generally, both positive and negative ion spectra and images were acquired for each sample. The spectra were acquired from a 100 × 100 μm^2 analysis area while the imaging areas were varied (25 × 25–500 × 500 μm^2) according to the experimental requirement. Each positive ion spectra were calibrated using CH_3^+ (m/z 15.023), $C_2H_3^+$ (m/z 27.023), $C_3H_5^+$ (m/z 41.039) and $C_7H_7^+$ (m/z 91.054) peaks. The negative ion spectra were calibrated using CH^- (m/z 13.007), C_2H^- (m/z 25.007) $COOH^-$ (m/z 44.997) and C_4H^- (m/z 49.007) peaks. Calibration errors were kept below 15 ppm in all the cases. Mass resolution (m/Δm) for typical spectra ranged between 7000 and 9000, calculated at m/z 44.997 ($COOH^-$) for negative ions and m/z 41.039 ($C_3H_5^+$) for positive ions respectively. All spectra and images were acquired by setting the primary ion dose density below the static limit (1×10^{13} ions/cm^2). Spectra and images from multiple points (≥3) on each sample were acquired and care was taken to use a new sample area for each analysis. The field of view is given in figure legends.

2.5. Immobilisation of phosphoprotein on gallium-treated ppAAc/ppAAm patterns for surface chemical analysis

Plasma polymer-coated silicon wafers were immersed for 5 min in either an aqueous solution of 20 mM gallium nitrate (pH ~ 2.6) or in a 20 mM solution of gallium nitrate made up in Solvent A (0.1 M sodium acetate/1 M NaCl, pH ~ 3.8) [24]. The metal ion-treated samples were then washed for 10 s in weak nitric acid (pH ~ 2.6) or Solvent A, and then washed for 10 s in Solvent B (33.3/33.3/33.3/0.1 vol% ddH_2O/acetonitrile/methanol/acetic acid) [9]. The gallium primed patterns were then immersed in PLS-BSA solution (2 μg ml^{-1} of protein in Solvent B) for 10 min [25], washed briefly in

Solvent B and then dried in a nitrogen stream. The rapid wash and incubation times were designed to reduce any solvent damage to the plasma polymer micropatterns. Visually it was observed that long exposure (~3–4 min) of micropatterns containing ppAAm to solvent B resulted in delamination of these films, while ppAAc and ppTG polymer chemistries remained physically stable.

2.6. Immobilisation of phosphoprotein on gallium-treated ppAAc for ELISA analysis

Glass coverslips coated with ppAAc were washed with Solvent A (0.1 M sodium acetate/1 M NaCl, pH 3.8), and then incubated for 60 min at 4 °C in a 20 mM solution of gallium (III) nitrate made up in Solvent A. After metal ion immobilisation, the samples were then washed with Solvent A and then with Solvent B. The test protein, PLS-BSA, was made up at 2 μg ml^{-1} in Solvent B and the gallium-treated ppAAc samples immersed in the solution for 60 min at room temperature. Finally, samples were then washed five times with Solvent B and then washed five times with a pH4 citrate buffer (0.15 M) prior to analysis in the ELISA assay.

2.7. Determination of surface protein binding using ELISA

The ELISA experiment was carried out using an anti-phosphoserine-BSA antibody-HRP conjugate (Abcam ab9334) raised against PLS-BSA. PLS-BSA is BSA functionalised with up to 30 O-phospho-L-serine molecules and contains a subfraction of non-functionalised BSA. The antibody specifically recognizes both free-phosphoserine, serine-phosphorylated peptide and proteins, and readily reacts to known phosphoproteins such as phosvitin and alpha casein (Abcam ab9334 product literature). The anti-phosphoserine-BSA antibody does not react with standard un-phosphorylated BSA and BSA is used as a blocking agent for this experiment.

ELISA experiments were carried out using standard protocols. Briefly, after contact with PLS-BSA surfaces were rinsed with and then incubated overnight at 4 °C with a blocking solution consisting of pH4 citrate buffer (0.15 M) containing 3% bovine serum albumin and 0.1% Tween 20. Samples were then washed with pH4 citrate buffer (0.15 M, pH4) and then incubated with 1 μg ml^{-1} anti-phosphoserine antibody (citrate buffer containing 0.5% human serum albumin). The samples were then washed with citrate buffer and the substrate added (4 mg of 2,2-Azino-bis(3-ethyl benzothiazoline-6-sulfonic acid) diammonium salt (ABTS) in 12 ml of citrate Buffer (0.1 M trisodium citrate pH 4) with 10 μl of H_2O_2 (30 vol% in H_2O)). Samples were removed from the solution and the solution optical density measured at 405 nm using a Biotek ELx800 plate reader.

3. Results and discussion

3.1. ToF-SSIMS imaging of micropatterns of plasma polymerised acrylic acid (ppAAc) and allylamine (ppAAm)

Previous work has suggested that in order to help protein adsorption and to suppress ion-ion interactions, buffers should contain high (>0.5 M) concentration of salt [26]. However for the case of the adsorption of phosphopeptides to gallium ions, the presence of NaCl may not decrease non-specific binding and it has been found that minimising ionic buffer strength improves IMAC-based phosphopeptide recovery [9]. Since the charge distribution on the surface of ppAAc also depends on the solvent, initial studies focussed on examining how the distribution of gallium ions was affected by the composition of the loading buffer. As ToF-SSIMS allows the identification of chemical species by mass, this allows not only an assessment of the patterned surface but also allows the position, for example, of the cations and anions from a metal salt solution co-localised on the pattern to be identified.

An alternating pattern made up of ppAAc/ppAAm was synthesised and Fig. 1 shows both positive (Fig. 1a) and negative (Fig. 1b) ion ToF-SSIMS images. The results demonstrate the distribution of secondary ion fragments characteristic of the plasma polymers acrylic acid (ppAAc) and allylamine (ppAAm). Major molecular fragments, which were indicative of individual plasma polymers, are listed in Table 1. The images show good transfer of the pattern from the original optical photomask template, with chemical and spatial resolution (~5 μm based on 80:20 intensity cut-off definition calculated on CN^- image shown in Fig. 1b) and sharp polymer interfaces and little evidence for the spill over from one chemical region into the other, illustrating the efficacy of the photolithography masking method. The results also clearly indicate that this patterning technique prevented reactions between the two strongly interacting chemistries, acrylic acid and allylamine [27].

Fig. 1c, d show a selection of positive and negative ToF-SSIMS images from a ppAAc/ppAAm micropattern pretreated with either 20 mM gallium nitrate made up in Solvent A (0.1 M sodium acetate/1 M NaCl, pH ~3.8) or water (pH ~2.6). Use of Solvent A introduces a significant amount of sodium on the plasma polymer films. As Na^+ can effect ion yields in ToF-SSIMS due to matrix effects [29], it is difficult to quantitatively interpret data where there are high intensity ions related to the salts. In Fig. 1c, the localisation of the gallium species is demonstrated using positive ion species corresponding to gallium at m/z 68.93 (the matching isotope was also detected at m/z 70.93). A line scan across the image (Fig. 1c) clearly shows a high background signal (~120 counts per pixel (cpp)) confirming that even though Ga localises preferentially on ppAAc, there is considerable secondary ion yield from the ppAAm regions. This may be due in part to the presence of a high concentration of sodium chloride (1 M) in Solvent A which would shield the positive

Table 1
Examples of charged species used for identification in ToF-SSIMS imaging. The assignments for species associated with amino acids were taken from the literature [28].

	ToF-SSIMS species	Mass (m/z)
Poly(acrylic acid), ppAAc	$C_2H_3O^+$	43.018
	$C_2H_4O^+$	44.026
	CHO_2^+	44.998
	CHO_2^-	44.998
Poly(allylamine), ppAAm	$C_3H_4N^+$	54.034
	$C_3H_8N^+$	58.066
	CN^-	26.003
Poly(tetraglyme), ppTG	$C_3H_7O^+$	59.049
Cysteine	$C_2H_6NS^+$	76.022
Methionine	$C_2H_5S^+$	61.011
Valine	$C_4H_{10}N^+$	72.081
Leucine	$C_5H_{12}N^+$	86.097
Proline	$C_4H_6N^+$	68.050
Threonine	$C_4H_5O^+$	69.034
Protein	S^-	31.972
	COS^-	59.967
	CNO^-	41.998
	SO_4^-	95.951
gallium	$^{69}Ga^+$	68.926
	$^{71}Ga^+$	70.924
	$^{69}GaH_2O^+$	86.936
	$^{71}GaH_20^+$	88.934
	$^{69}GaO^-$	84.920
	$^{71}GaO^-$	86.918
	$^{69}GaO_2^-$	100.915
	$^{71}GaO_2^-$	102.913
	$^{69}GaPO_3^-$	147.884
	$^{69}GaPO_4^-$	163.879

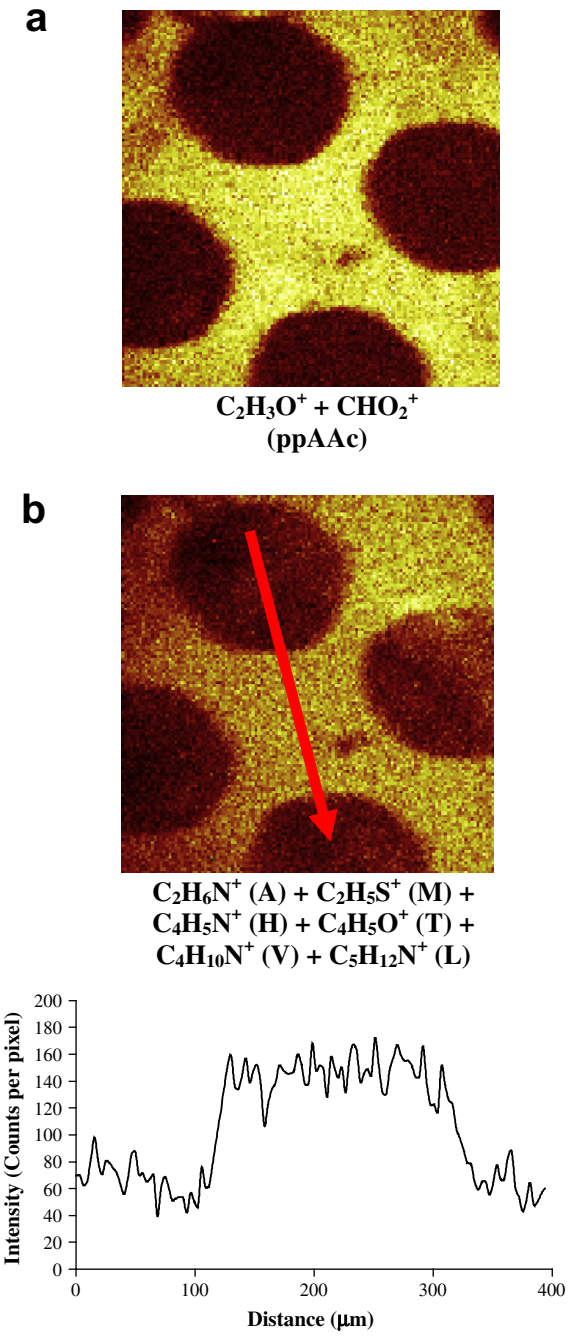

Fig. 2. (a) and (b) ToF-SSIMS images of chemically complex ppAAc/ppAAm micropatterns pretreated with gallium nitrate and then treated with phosphoprotein PLS-BSA (see text for experimental details). (Field of view 500 × 500 μm.) The line scans shown below represent the intensity variation along the red arrows superimposed on the TOF-SSIMS images, both with respect to the length and the direction.

charge on the ppAAm region. This charge shielding may result in an increase in binding of Ga onto the ppAAm areas. This conclusion is further supported by data in Fig. 1d, where 20 mM gallium nitrate was prepared in water (pH ~2.6) with negligible gallium detected on the ppAAm area. The nitrate counterion was identified in Fig. 1d by NO_3^-, and demonstrates that this anion binds to the positively charged ppAAm areas, but not to the ppAAc areas. These results clearly demonstrate specific ions can be directed from solution to different surface regions in a micropattern using combinations of appropriate plasma polymers and solvents.

3.2. ToF-SSIMS imaging of proteins bound to micropatterns containing both ppAAc and ppAAm

To investigate the capacity of these chemistries to form metal affinity surfaces and to bind phosphoproteins, patterns of ppAAc/ppAAm were prepared. Fig. 2 shows ToF-SSIMS from ppAAc/ppAAm patterns treated initially with gallium nitrate solution and followed by treatment with PLS-BSA. Although in section (1) it was demonstrated that aqueous buffer provided a cleaner TOF-SSIMS image compared to NaCl buffer, Solvent A was employed for gallium loading as it was adapted from IMAC literature and has been shown in previous studies to be necessary for the gallium-phosphate selectivity.

Fig. 2a shows the spatially defined chemical patterns produced with ppAAc and ppAAm. The ions associated with protein, namely $C_2H_6N^+$ (alanine), $C_2H_5S^+$ (methionine), $C_4H_5N^+$ (histidine), $C_4H_5O^+$ (threonine), $C_4H_{10}N^+$ (valine) and $C_5H_{12}N^+$ (leucine), are more intense on the gallium-ppAAc region. A line scan across the sample in Fig. 2b shows that there is some protein-related signal in the ppAAm regions of the sample. The signals detected for what is apparently protein on the ppAAm regions is of a low intensity. The signal mostly comes from $C_2H_6N^+$, a species that is associated not only with the amino acid alanine, but also arises from the ppAAm surface itself. Even after a comparison of the ToF-SSIMS spectra with a spectra from a pure ppAAm sample (data not shown), it was not possible to completely resolve some of the nitrogen-containing species arising from protein and from those due to the ppAAm surface. The yields of nitrogen-containing secondary ion fragments from both protein and ppAAm surface give rise to the high background signal seen on the intensity line scan shown in Fig. 2b. Nevertheless the line scans also show a 80cpp increase in signal between ppAAm (average secondary ion intensity ~80 units) and ppAAc (average secondary ion intensity ~ 160 units) when amino acid secondary ion fragment yields were spatially mapped across the sample surface. These results suggest that the carboxylic acid moieties on ppAAc have the ability to create an immobilised metal affinity (IMA) surface that would appear to replicate the behaviour seen with NTA and IDA, but that the amine moieties found in ppAAm do not appear to display properties typically associated with amine-based IMA systems, i.e. tris(carboxymethyl)ethylenediamine (TED). This may be due in part to the fact that the solvent conditions have not been optimised in this study for metal affinity on ppAAm. However, it has been observed that TED forms weaker IMAC protein adsorbents than IDA, which may also partly explain this observation [6].

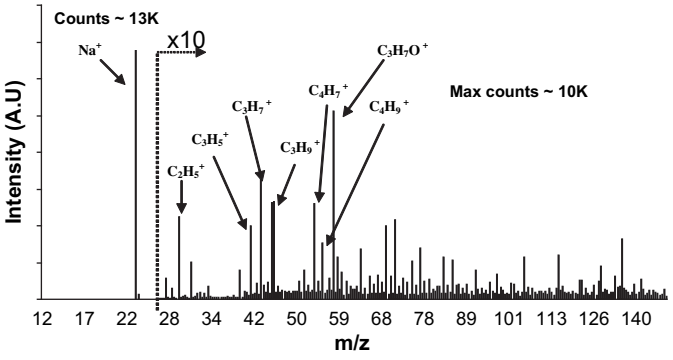

Fig. 3. Positive ion ToF-SSIMS mass spectrum for m/z 0–100 representing the difference in the spectra for ppTg before and after photolithographic patterning.

3.3. ToF-SSIMS imaging of proteins bound to micropatterns containing gallium-treated plasma polymerised acrylic acid (ppAAc) and tetraglyme (ppTG)

To enable a specific examination of the phosphoprotein binding of gallium-treated ppAAc, a micropattern consisting of ppAAc on a protein resistant background made from plasma polymerised tetraglyme (ppTG) was prepared. To determine whether the surface chemistry of the ppTG was damaged during the photolithographic patterning, the surface chemistry was examined before and after the procedure using X-ray Photoelectron Spectroscopy (XPS). It was found that there was a slight increase in hydrocarbon content after the photolithography treatment (data not shown). The same examination was performed using ToF-SSIMS in order to obtain a better understand of the contamination. Fig. 3 represents differences in the ToF-SSIMS spectra for ppTg before and after photolithographic patterning. It is apparent from the ToF-SSIMS spectrum that the bulk of the peaks are associated with hydrocarbon fragments (e.g. $C_2H_5^+$, $C_3H_7^+$, etc), correlating with the XPS data. Additionally, there was evidence of an increase in sodium at the surface after photolithography that is due to the use of the alkaline developer. Interestingly, as shown in Fig. 4, the presence of this small level of hydrocarbon does not appear to affect the ability of the ppTG surface to resist protein adsorption.

Fig. 4 shows a mixture of positive and negative ToF-SSIMS images from a ppTG/ppAAc micropattern and demonstrates that the pattern is chemically resolved. The major positive and negative molecular fragments used to carry out this analysis are listed in Table 1. The micropattern was treated with gallium nitrate in solvent A and then subsequently with the model phosphoprotein, PLS-BSA. Fig. 4 shows that the secondary ion molecular fragments associated with gallium (Fig. 4b, d) and PO_3^- (Fig. 4d) were co-

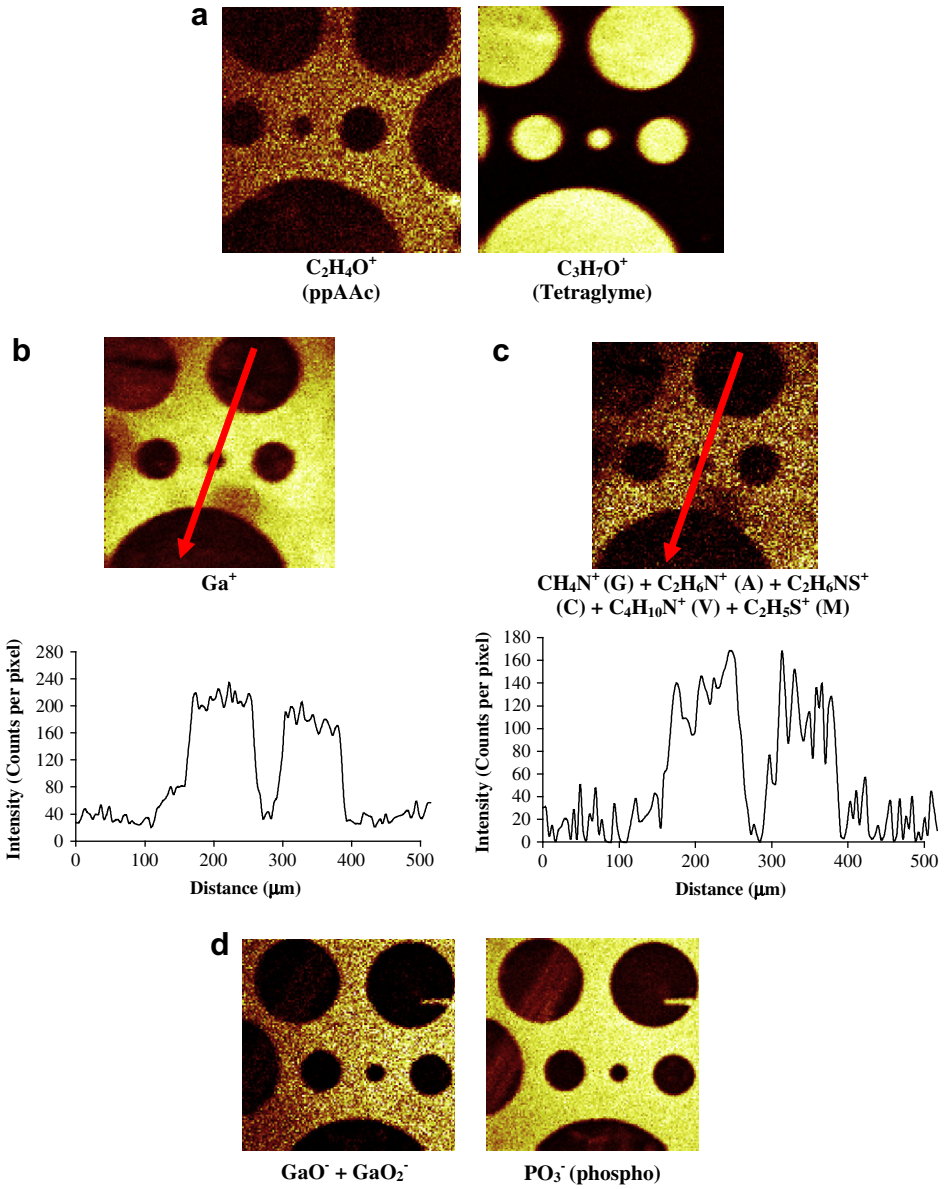

Fig. 4. ToF-SSIMS images of ppTG/ppAAc micropatterns with gallium nitrate and phosphoprotein PLS-BSA (see text for experimental details). (Field of view 500 × 500 μm.) (a) positive secondary ion charged species associated with plasma polymers, (b) positive secondary ion charged species associated with gallium, (c), positive secondary ion charged species associated with protein, and (d) negative secondary ion charged species associated with phosphates and gallium. The line scans represent the intensity variation along the red arrows superimposed on the TOF-SSIMS images, both with respect to the length and the direction.

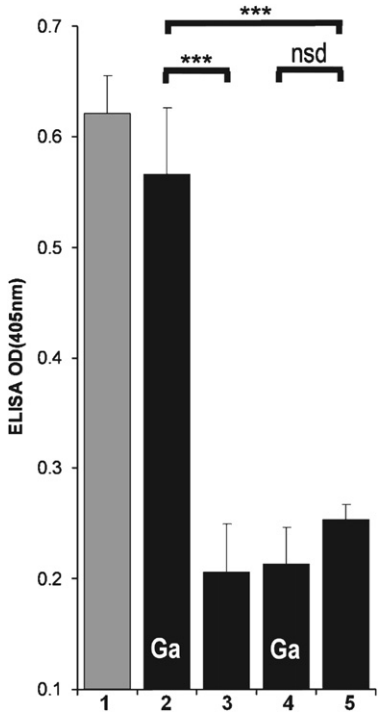

Fig. 5. Amount of PLS-BSA immobilised to plasma polymer ppAAc under different conditions, as assessed using an anti-phosphoprotein antibody ELISA test (see text); 1. protein covalently immobilised on ppAAc using an EDC/NHS; 2. ppAAc pretreated with gallium ions treated with phosphoprotein at pH4; 3. ppAAc with no gallium ions treated with phosphoprotein at pH4; 4. ppAAc pretreated with gallium ions treated with phosphoprotein at pH8; 5. ppAAc with no gallium ions treated with phosphoprotein at pH8; The data has been tested by Student's *t*-test where $n = 6$, $^{***}p < 0.001$ and nsd = no significant difference.

localise with ppAAc chemistry. These images provide conclusive evidence for complexes formed between species associated with both gallium and phosphate such as $^{69}GaPO_3^-$ and $^{69}GaPO_4^-$. The single ion images from these two fragments have been summed in the image due to their low secondary ion yields, but nonetheless the localisation of these secondary ion correlate with the ppAAc regions. Interestingly, the data also indicates that the ppTG chemistry present on the surface (represented by $C_3H_7O^+$ secondary ion image Fig. 4a) inhibits localisation of Ga metal species under these experimental conditions (see the line scan in Fig. 4b).

The distribution of species associated with protein-related amino acid secondary ion fragments are shown in Fig. 4c. This figure demonstrates the summed counts from glycine (CH_4N^+), methionine ($C_2H_5S^+$), cysteine ($C_2H_6NS^+$), alanine ($C_2H_6N^+$) and valine ($C_4H_{10}N^+$) ions and clearly demonstrates the co-localisation of the proteins on the gallium modified ppAAc surfaces. From the line scan presented (Fig. 4c), it is clear that the intensity drops to 0 at a distance of approx. 280 μm. This corresponds to the small circular region of ppTG located in the centre of the figure. These results indicate that the ppAAc surface is able to specifically bind protein via an affinity for the immobilised metal, where a high degree of spatial resolution is possible. Fig. 4c also confirms that the ppTg has retained its non-fouling properties despite the presence of contaminants as shown in Fig. 3.

3.4. ELISA assessment of the ability of gallium ion-treated ppAAc to bind a phosphoprotein

Fig. 5 illustrates results for ELISA experiments developed to biochemically investigate how different solvent conditions affected the ability of the ppAAc-modified surface to bind the phosphoprotein PLS-BSA and the influence of the addition of a second protein to the mixture, fibrinogen. A positive control is shown in column 1, and represents the ELISA signal for the same solution concentration of PLS-BSA when it is able to covalently attach to the ppAAc surface via N-(3-dimethylaminopropyl)-N′-ethyl-carbodiimide/N-hydroxysuccinimide (EDC/NHS) chemistry. When gallium ions are present on the ppAAc surface and the phosphoprotein is introduced using Solvent B (33.3/33.3/33.3/0.1 vol% ddH_2O/acetonitrile/methanol/acetic acid) (Fig. 5, column 2), similar amounts of protein were immobilised as in the positive control sample (Fig. 5, column 1). When gallium ions were not present (Fig. 5, column 3) only background levels of protein were detected, and similar low level interactions are seen when the PLS-BSA is introduced to the gallium-ppAAc surface in aqueous buffer at pH8 instead of solvent B (Fig. 5, columns 4 and 5). There was no significant difference seen when comparing the data presented in columns 4 and 5, indicating that there was no difference in the protein binding capacity of the gallium pretreated and pure ppAAc surfaces under these sub-optimal conditions.

In order to determine whether the gallium-ppAAc surface can selectively immobilise a phosphoprotein in the presence of other proteins, the surface was exposed to a 1:10,000 mixture of PLS-BSA and fibrinogen and the protein capture compared to that from solutions with 2 μg ml^{-1} PLS-BSA or 20 mg ml^{-1} fibrinogen alone (Fig. 6). The saturated fibrinogen solution gave a background signal with the anti-phosphoserine-BSA antibody (Fig. 6, column 2). However, the presence of excess fibrinogen did not affect the immobilisation of the PLS-BSA as can be seen by comparison of columns 1 and 3 in Fig. 6. The signal intensity of column 1 should however be the same as column 3 if the gallium-treated ppAAc is able to selectively immobilise phosphoprotein without influence from the other proteins in the

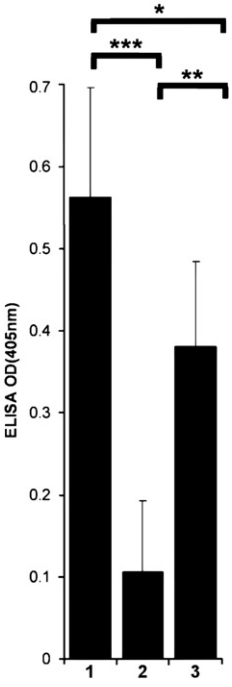

Fig. 6. Selective immobilisation of a phosphoprotein onto the gallium-ppAAc surface in the presence of other proteins, as assessed using an anti-phosphoprotein antibody ELISA test (see text); 1. mixture of 2 μg ml^{-1} PLS-BSA and 20 mg ml^{-1} fibrinogen (concentration of 1:10,000); 2. 20 mg ml^{-1} fibrinogen (background); 3. 2 μg ml^{-1} PLS-BSA; The data has been tested by Student's *t*-test where $n = 6$, $^{*}p < 0.05$, $^{**}p < 0.01$, and $^{***}p < 0.001$.

mixture. It is apparent that the intensity obtained from the mixture (column 1) is offset from the measurement for the pure phosphoprotein solution (column 3) by a similar amount obtained for the background measurement (column 2). Therefore in the competitive solution experiment, there is some non-specific binding of the fibrinogen at background intensity levels. Despite this, the results clearly demonstrate that ppAAc treated with gallium ions preferentially immobilises PLS-BSA even in the presence of an excess of a competing protein.

In a final set of experiments, surfaces were washed with buffers of a high pH (100 mM ammonium chloride, pH 10). This removed all protein and gallium- related molecular ions from the ToF-SSIMS images, whilst leaving the plasma polymer pattern intact (data not shown). As such, these results confirm that under these experimental conditions, the retained protein could be recovered from the surface. This indicates these surfaces have the potential for use in microfludic devices, enabling rapid isolation or pre-concentration of phosphopeptides or phosphoproteins (or similar protein-metal ion complexes) from a mixture prior to mass spectrometric or other analysis techniques. Future work is necessary to confirm the performance of these surfaces with more complex solutions such as a cell lysate peptide mixture if they are to be successfully implemented in an IMAC like application. In addition, a more detailed study of the regeneration and lifetime of the surfaces would be necessary.

4. Conclusions

ToF-SSIMS imaging has been utilised to visualise the chemical specificity and selectivity of surface micropatterns fabricated from a range of plasma polymers. This technique was employed as it provided the necessary spatial resolution to chemically resolve the multiple components present within these systems. In addition, the biological specificity of these surfaces was examined using ELISA. The results clearly demonstrate that under the correct solvent conditions, plasma polymerised thin films of acrylic acid (ppAAc) can coordinate gallium and are able to selectively attract phosphoproteins. Analysis of the ToF-SSIMS and ELISA data both indicate that the ionic strength and pH of the buffer were vital for surface sensitivity and selectivity. In fact, by raising the pH of the buffer it is possible to disassociate the protein-metal complex from the surface, regenerating the original plasma polymer surface chemistry. These results, combined with the fact that plasma polymers can be readily applied to virtually any solid substrate, make this a surface modification strategy that can be readily integrated into microfludic devices. These surface micropatterns have the potential to be implemented in applications involving the rapid isolation or pre-concentration of phosphopeptides/proteins prior to mass spectrometry or other analysis techniques.

Acknowledgements

The authors would like to thank the EPSRC for project funding. We acknowledge NESAC/Bio for use of the NESAC/Bio toolbox which is funded by NIH grant EB-002027.

References

[1] Favia P, Sardella E, Gristina R, d'Agostino R. Surface and Coatings Technology 2003;169–170:707.
[2] McArthur SL. Surface and Interface Analysis 2006;38(11):1380–5.
[3] Siow K, Britcher L, Kumar S, Griesser H. Plasma Processes and Polymers 2006;3(6–7):392–418.
[4] Salim M, Mishra G, Fowler GJS, O'Sullivan B, Wright PC, McArthur SL. Lab on a Chip 2007;7(4):523–5.
[5] Sun T, Norton D, Vickers N, McArthur SL, Mac Neil S, Ryan AJ, et al. Biotechnology and Bioengineering 2008;99(5):1250–60.
[6] Porath J. Protein Expression and Purification 1992;3(4):263–81.
[7] Delom F, Chevet E. Proteome Science 2006;4:12.
[8] Barnouin KN, Hart SR, Thompson AJ, Okuyama M, Waterfield M, Cramer R. Proteomics 2005;5:4376–88.
[9] Ndassa YM, Orsi C, Marto JA, Chen S, Ross MM. Journal of Proteome Research 2006;5(10):2789–99.
[10] Cuccurullo M, Schlosser G, Cacace G, Malorni L, Pocsfalvi GJ. Mass Spectrometry 2007;42:1069–78.
[11] Pinkse MWH, Uitto PM, Hilhorst MJ, Ooms B, Heck AJR. Analytical Chemistry 2004;76(14):3935–43.
[12] Hoffmann R, Reichert I, Wachs WO, Zeppezauer M, Kalbitzer HR. International Journal of Peptide and Protein Research 1994;44(3):193–8.
[13] Qasim MA, Ranjbar MR, Wynn R, Anderson S, Laskowski Jr M. Journal of Biological Chemistry 1995;270(46):27419–22.
[14] Ibanez AJ, Muck A, Svatos A. Journal of Proteome Research 2007;6:3842–8.
[15] Li J, LeRiche T, Tremblay T-L, Wang C, Bonneil E, Harrison DJ, et al. Molecular & Cellular Proteomics 2002;1(2):157–68.
[16] Zhou L, Wang K, Tan W, Chen Y, Zuo X, Wen J, et al. Analytical Chemistry 2006;78(17):6246–51.
[17] Wen J, Yang X, Wang K, Tan W, Zhou L, Zuo X, et al. Biosensors and Bioelectronics 2007;22(11):2759–62.
[18] Cooper KR, Elster J, Jones M, and Kelly RG. Optical fiber-based corrosion sensor systems for health monitoring of aging aircraft. AUTOTESTCON Proceedings, 2001. IEEE Systems Readiness Technology Conference, 2001. p. 847–856.
[19] Whittle JD, Short RD, Douglas CWI, Davies J. Chemistry of Materials 2000;12(9):2664–71.
[20] O'Toole L, Beck AJ, Short RD. Macromolecules 1996;29(15):5172–7.
[21] Löpez G, Ratner B, Tidwell C, Haycox C, Rapoza R, Horbett T. Journal of Biomedical Materials Research 1992;26(4):415–39.
[22] Bullett NA, Talib RA, Short RD, McArthur SL, Shard AG. Surface and Interface Analysis 2006;38:1109–16.
[23] Goessl A, Garrison MD, Lhoest J, Hoffman AS. Journal of Biomaterials Science Polymer Edition 2001;V12(7):721.
[24] Hemdan ES, Porath J. Journal of Chromatography 1985;323(2):247–54.
[25] Zachariou M, Traverso I, Hearn MTW. Journal of Chromatography 1993;646:107–20.
[26] Porath J. Abstracts of Papers of the American Chemical Society 1992;203:86. ANYL.
[27] Beck AJ, Whittle J, Bullett N, Eves P, Mac Neil S, McArthur S, et al. Plasma Processes and Polymers 2005;2(8):641–9.
[28] Wagner MS, McArthur SL, Shen MC, Horbett TA, Castner DG. Journal of Biomaterials Science-Polymer Edition 2002;13(4):407–28.
[29] Léonard D, Mathieu HJ. Fresenius' Journal of Analytical Chemistry 1999;365(1):3–11.